Loss of p63 and its microRNA-205 target results in enhanced cell migration and metastasis in prostate cancer

Paola Tucci[a,b,1], Massimiliano Agostini[a,1], Francesca Grespi[a,c,d,1], Elke K. Markert[e], Alessandro Terrinoni[f], Karen H. Vousden[g], Patricia A. J. Muller[g], Volker Dötsch[h], Sebastian Kehrloesser[h], Berna S. Sayan[i], Giuseppe Giaccone[j], Scott W. Lowe[k], Nozomi Takahashi[c,d], Peter Vandenabeele[c,d], Richard A. Knight[a], Arnold J. Levine[e], and Gerry Melino[a,c,f,2]

[a]Medical Research Council, Toxicology Unit, Leicester University, Leicester LE1 9HN, United Kingdom; [b]Department of Pharmaco-Biology, University of Calabria, 87036 Rende (Cosenza), Italy; [c]Department of Molecular Biomedical Research, Flanders Institute for Biotechnology, B-9052 Ghent, Belgium; [d]Department of Biomedical Molecular Biology, Ghent University, B-9000 Ghent, Belgium; [e]Institute for Advanced Study, Princeton, NJ 08540; [f]Biochemistry Laboratory, Istituto Dermopatico dell'Immacolata, Istituto di Ricovero e Cura a Carattere Scientifico and University of Rome "Tor Vergata," 00133 Rome, Italy; [g]The Beatson Institute for Cancer Research, Glasgow G61 1BD, United Kingdom; [h]Institute of Biophysical Chemistry and Center for Biomolecular Magnetic Resonance, Goethe University, 60438 Frankfurt, Germany; [i]University of Southampton, Faculty of Medicine, Cancer Sciences Unit, Somers Cancer Research Building, Southampton SO16 6YD, United Kingdom; [j]Medical Oncology Branch, National Cancer Institute, National Institutes of Health, Bethesda, MD 20892; and [k]Memorial Sloan-Kettering Cancer Center, New York, NY 10065

Edited by Carol Prives, Columbia University, New York, NY, and approved August 2, 2012 (received for review July 8, 2011)

p63 inhibits metastasis. Here, we show that p63 (both TAp63 and ΔNp63 isoforms) regulates expression of miR-205 in prostate cancer (PCa) cells, and miR-205 is essential for the inhibitory effects of p63 on markers of epithelial–mesenchymal transition (EMT), such as ZEB1 and vimentin. Correspondingly, the inhibitory effect of p63 on EMT markers and cell migration is reverted by anti–miR-205. p53 mutants inhibit expression of both p63 and miR-205, and the cell migration, in a cell line expressing endogenous mutated p53, can be abrogated by pre–miR-205 or silencing of mutated p53. In accordance with this in vitro data, ΔNp63 or miR-205 significantly inhibits the incidence of lung metastasis in vivo in a mouse tail vein model. Similarly, one or both components of the p63/miR-205 axis were absent in metastases or colonized lymph nodes in a set of 218 human prostate cancer samples. This was confirmed in an independent clinical data set of 281 patients. Loss of this axis was associated with higher Gleason scores, an increased likelihood of metastatic and infiltration events, and worse prognosis. These data suggest that p63/miR-205 may be a useful clinical predictor of metastatic behavior in prostate cancer.

tumorigenesis | apoptosis | E-cadherin | PC3 cell | DU145 cell

The p63 protein is a homolog of the p53 tumor suppressor gene and the linear descendant of the most ancient member of the p53 family (1, 2). Because of the presence of two promoters, p63 encodes two major classes of proteins: those containing (TAp63) and those lacking (ΔNp63) an N-terminal transactivating (TA) domain homologous to that present in p53 (1). ΔNp63 isoforms can inhibit the transcriptional activity of the TA isoforms, both by competing for consensus promoter elements or by heterodimerization. In addition, alternative splicing at the C terminus generates at least three further isoforms (α, β, and γ) of both TAp63 and ΔNp63. ΔNp63α via a second C-terminal TA domain can transactivate a spectrum of genes distinct from that recognized by the N-terminal TA domain. Here, we investigated the possibility that this transcription factor exerts at least part of its cancer-related effects (3) by also activating expression of small noncoding RNA sequences such as microRNAs (miRs) (4, 5).

A major problem of human cancer is the occurrence of metastatic spread. Cells within the primary lesion undergo epithelial–mesenchymal transition (EMT), which results in increased cell motility and migration, and which is associated with increased expression of ZEB1, SIP1, and N-cadherin and with reduced expression of E-cadherin. Recently, some of these EMT proteins have been shown to be targeted by miRs, and miRs may

thus play a role in EMT and metastasis (6). For example, expression of the miR-200 family, and miR-205, have been shown to be reduced in models of EMT (7) and act, at least partially, by directly targeting the 3′ UTRs of ZEB1 and SIP1. MiR expression profiling has also identified the miR-200 family and miR-205, as well as others, whose expression is selectively reduced in breast cancer metastases, but not in those of colon, bladder, or lung (8). MiR-205 has also been shown to suppress clonogenicity of MCF-7 breast cancer cells and, importantly, to suppress metastatic spread of a human breast cancer xenograft in nude mice (9). MiRs, including a reduction in miR-205, have also been implicated in prostate cancer (PCa) (10), and their expression levels correlated with staging, metastasis, and androgen dependence. In addition to its function in the regulation of EMT, the loss of miR-205 in prostate cancer has also been related to reduced expression of the tumor suppressor genes, IL24 and IL32 (11).

In the present study, we show that miR-205 expression is regulated by both TAp63 and ΔNp63, and that both p63 and miR-205 are lost in human prostate cancer metastasis. The effects of p63 on ZEB1 and on the expression of epithelial and mesenchymal markers are mediated through miR-205 and p53 mutations, because mutant p53 can suppress the actions of p63. The significance of this p63/miR-205 axis has been confirmed in mouse metastasis models and in human clinical samples. These data suggest that both p63 and miR-205 may both have diagnostic potential as biomarkers of metastasis in prostate cancer and provide unique therapeutic targets in this common malignancy.

Results

TAp63 and ΔNp63 Drive the Expression of miR-205. Although p63, and particularly the ΔNp63α isoform, is highly expressed in the basal layer of normal prostatic epithelium, and is required for the development of secretory cells, p63 is undetectable in the vast

Fig. 1. ΔNp63 regulates ZEB1 through its target miR-205. (A) PC3 cells were transfected for 48 h to express HA-ΔNp63 and endogenous miR-205 levels assessed by qRT-PCR. Expression level of p63 is shown in the Western blot (WB). (B) miR-205 levels in A431 cells transfected with a mixture of three validated siRNAs targeting different parts of p63. (C) ΔNp63α–PC3-Tet–On cells or ΔNp63α–PC3–Tet–On cells expressing anti–miR-205, were treated with 1 μg/mL doxycycline (Doxy) for 24 h and miR-205 was assessed by qRT-PCR. Induction of p63 is shown in the WB. (D) Insertion of miR-205 promoter region in a luciferase reporter gene leads to increased luciferase activity in the presence of ΔNp63 in SaOS-2 cells. Mutation of the RE-III p53-binding site abolished ΔNp63-mediated luciferase activity. (E) Chromatin immune precipitation (ChIP) experiment that shows that p63 is able to bind the p53RE-II and p53RE-III sites. (F) ZEB1 protein levels in miR-205–PC3–Tet–On cells. Percentage of inhibition of ZEB1 protein is expressed relative to untreated miR-205–PC3–Tet–On cells and normalized to GAPDH levels. (G) qRT-PCR and WB of ZEB1 levels in PC3 cells transfected for 48 h as indicated. (H) WB of ZEB1 protein in PC3 cells transfected with HA-ΔNp63, and subsequently transfected with anti–miR-205 or a negative control (Neg Ctrl). Percentage of inhibition of ZEB1 protein is expressed relative to pcDNA plus Neg Ctrl and normalized to actin levels. All of the qRT-PCR results were normalized to RNU6B or GAPDH and data represent mean ± SD of three different experiments analyzed in triplicate. Levels of actin or GAPDH were used as loading control.
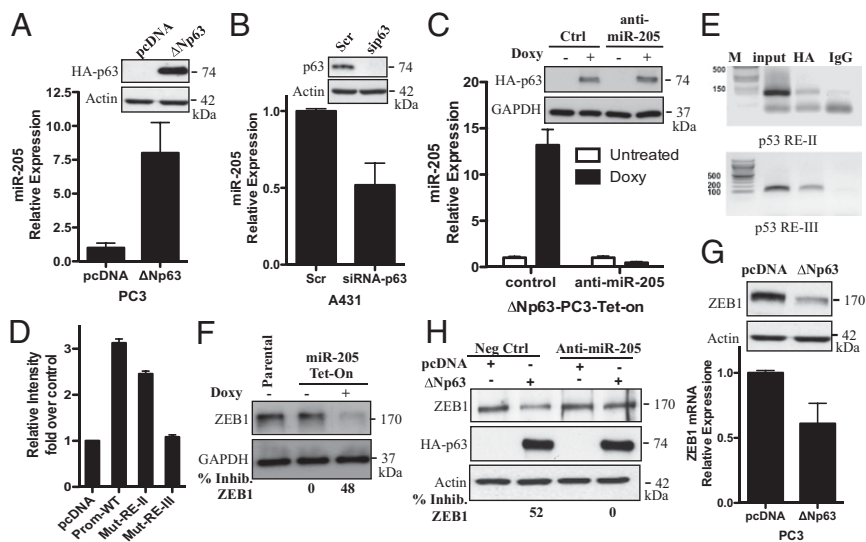
majority of androgen-dependent (VcaP and LNCaP) and androgen-independent (DU145 and PC3) prostatic cancer cell lines. Similarly, miR-205 is expressed in normal prostate but not in prostatic cancer cell lines. To investigate whether this association was due to a functional relationship between ΔNp63 and miR-205, we transiently expressed ΔNp63 in PC3 cells, which resulted in an 8-fold increase in miR-205 expression (Fig. 1A). Because prostatic cancer cells do not express p63, we used p63 positive-A431 cells to assess whether knockdown of p63 reduced miR-205 expression. Transient overexpression of sip63 indeed reduced miR-205 levels by 50% (Fig. 1B). To confirm the ability of p63 to modulate miR-205, we transiently transfected H1299 cells with either empty vector or vectors expressing either ΔNp63 or TAp63. Fig. S1 A and B show that the expression of miR-205 was induced by roughly 140-fold by ΔNp63, whereas TAp63 induced miR-205 by 21-fold. Next we used two distinct cell lines, MCF-7 cells that express mainly the ΔNp63 isoform (Fig. S1C) and MDA-MB231 cells (expressing only TAp63, Fig. S1E). Using p63 N-terminal–specific siRNA, we found that knockdown of ΔNp63 (MCF7 cells: Fig. S1D) and TAp63 (MDA-MB231 cells: Fig. S1F) reduced miR-205 expression. The induction of ΔNp63 by doxycycline in PC3–Tet–On (Fig. 1C) and in SaOS-2–Tet–On (Fig. S1G) cell lines resulted in a large induction of miR-205 transcripts that was completely abrogated by stable expression of an inhibitor of miR-205 (Fig. 1C). Because the time kinetics of miR-205 induction (3–6 h after ΔNp63 induction) were similar to those of known direct ΔNp63 targets such as K14 (Fig. S1 H and I), we explored whether miR-205 is a direct transcriptional target of ΔNp63.

We screened a region of ~2,000 bp upstream of the miR-205 transcriptional start site (TSS) for consensus p53 response elements (p53RE) by Matinspector. Three putative p53RE were identified (Fig. S1J): RE-I, located −953/−931 bp upstream of the TSS (core similarity = 1.0, matrix = 0.989), RE-II at −635/−613 (core similarity = 1.0, matrix = 0.800), and RE-III at −503/−481 (core similarity = 1.0, matrix = 0.919). This entire 2,000-bp region was cloned upstream of a luciferase reporter and cotransfected with ΔNp63 or empty vector in SaOS-2 cells. ΔNp63 transfection resulted in an approximately threefold enhancement of promoter activity (Fig. 1D, Prom-WT), suggesting that the 2,000-bp fragment indeed contains ΔNp63 binding sites. To determine which of the p53REs is bound by p63, we performed both chromatin

immunoprecipitation (ChIP) experiment and luciferase assay with mutated p53RE. p63 bounded both the p53RE-II and p53RE-III sites (Fig. 1E) but not p53RE-I, and loss of promoter activity was observed using the mutated p53RE-III (Fig. 1D, Mut-RE-III), thus demonstrating that p63 directly drives the miR-205 promoter via the two binding sites within 700 bp of the TSS.

p63 Targets ZEB1 Through miR-205. We next investigated the pathways regulated by miR-205. MiR-205 has been shown to impair the migratory and invasive properties of PCa cells through modulating the expression of EMT regulators (7, 12). Based on the fact that ΔNp63 drives the expression of miR-205, we asked whether the cellular levels of a miR-205 target, ZEB1 (7, 13), would also be affected by expression of ΔNp63. We confirmed previous evidence that miR-205 modulates ZEB1, using a miR-205–PC3-inducible cell line. The induction of the miR by adding doxycycline (Fig. S2A) resulted in a significant 48% reduction of ZEB1 protein expression level, compared with the untreated miR-205–Tet–On cells, Fig. 1F. Similarly, transient transfection of PC3 and H1299 cells with a miR-205 precursor resulted in a reduction of around 50% in ZEB1 levels, as detected both by qRT-PCR and Western blotting (Fig. S2 B and C). In addition, inhibition of miR-205 by anti–miR-205 in A431 cells resulted in an increase of about 50% of ZEB1 at both the mRNA and protein levels (Fig. S2D). We then performed Western blot analysis and qRT-PCR of ZEB1 levels in PC3 cells transiently transfected with ΔNp63 and found a significant reduction of ZEB1 at both protein and RNA levels (Fig. 1G). The same result was also found at the protein level in doxycycline-induced ΔNp63α–SaOS-2–Tet–On cells (Fig. S2E).

We then tested whether the modulation of ZEB1 expression by ΔNp63 required miR-205. To address this, we expressed ΔNp63 in PC3 cells in the presence or absence of anti–miR-205. Whereas ΔNp63 expression still resulted in reduced ZEB1 protein levels with the scrambled control, ZEB1 levels remained unchanged in the presence of anti–miR-205 (Fig. 1H). Again, the same result was obtained using the doxycycline-induced ΔNp63α–PC3–Tet–On cells transfected with anti–miR-205 (Fig. S2F).

Therefore, ΔNp63 represses ZEB1 expression through the direct activation of its target miR-205.

CELL BIOLOGY

p63 Affects the Expression of Epithelial and Mesenchymal Markers.
ZEB1 is a major regulator of EMT by reducing expression of epithelial proteins such as E-cadherin while increasing expression of mesenchymal markers such as vimentin. Therefore, the reduction in ZEB1 expression by ΔNp63 suggests that activation of the ΔNp63/miR-205 axis may induce a mesenchymal-to-epithelial transition (MET). To evaluate this, we assessed whether ΔNp63 and miR-205 affected E-cadherin and vimentin levels. Following transfection of ΔNp63 in PC3 cells, E-cadherin was increased at both mRNA and protein levels (Fig. 2*A*), whereas expression of vimentin was reduced (Fig. 2*B*). Similarly, transfection of pre–miR-205 also produced an increase in E-cadherin transcripts and protein (Fig. 2*C*), with a reduction in vimentin expression (Fig. 2*D*). Cotransfection of ΔNp63 with anti–miR-205 restored vimentin expression (Fig. 2*E*), showing that the effects of ΔNp63 on ZEB1 and its E-cadherin and vimentin targets are mediated by miR-205.

p63 Inhibits Cell Migration and Produces Changes in Golgi Polarization.
The repression of ZEB1 by ΔNp63, together with the changes in epithelial and mesenchymal markers, suggested that ΔNp63, acting through miR-205, may play an important role in cell morphology and migration and therefore in metastasis. To test this, we expressed ΔNp63 in PC3 cells and first observed a morphological change from a spindle-shaped mesenchymal form to a more rounded epithelium-like form, with many cells aggregating together in groups. Secondly, using a wound healing or scratch assay, we observed an inhibition of migration by cells overexpressing ΔNp63 compared with those transfected with the empty vector (Fig. S3*A* and Movies S1 and S2). Similar results were obtained following transfection of cells with pre–miR-205 (Fig. S3*B* and Movies S3 and S4). Conversely, inhibition of miR-205 in ΔNp63-transfected PC3 cells caused an increase in migration compared with cells transfected with ΔNp63 alone (Fig. 3*A* and Movies S5, S6, S7, and S8). qRT-PCR confirmed that miR-205 levels remained elevated throughout the duration of the scratch assays (Fig. S3*C*), without significant differences in cell cycle profile or in cell death between cells transfected with empty vector or with ΔNp63 (Fig. S3*D*).

Redistribution of the Golgi apparatus is an important event in the polarization and migration of many cell types. A polarized Golgi supplies membrane components for leading edge protrusion (14). We therefore investigated the effects of ΔNp63 expression in PC3 cells on Golgi polarization by immunofluorescence analysis. In PC3 cells transfected with an empty vector,

both the Golgi apparatus and actin filaments polarized to face the direction of migration when they moved toward the scratch wounds in a cell culture dish (Fig. 3 *B*, *Upper* and *C* and Fig. S4*A*, *Left*). Conversely, ΔNp63 cells did not consistently orientate their Golgi toward the wounded area (Fig. 3 *B*, *Lower* and *C* and Fig. S4*A*, *Right*), suggesting that their random migration may be associated with an inability to properly establish an axis of polarity with respect to the wound's edge. The same results were obtained using the ΔNp63–PC3–Tet–On (Fig. S4 *B* and *C*) and the miR-205–PC3–Tet–On (Fig. S4 *D* and *E*) cell lines in which the expression levels of ΔNp63 or miR-205, respectively, were induced by doxycycline. In addition fluorescence time-lapse imaging of GFP-spectrin revealed that migrating PC3 cells adopted a fan-like morphology with extended lamellipodia at the migration front and started to migrate toward the wound in an organized fashion (Fig. S4*F*, *Left* and Movie S9). However, in cells overexpressing ΔNp63, the spectrin filaments polarized randomly with an alternating protruding and retracting behavior (Fig. S4*F*, *Right* and Movie S10).

Taken together, ΔNp63, through the induction of miR-205, negatively regulates cell migration by modulating cell spreading and polarization.

p53 Mutants Inhibit p63 Activity. Recent studies have shown that p53 mutants can inhibit p63 (15, 16) and that this can enhance invasion by tumor cells (17–19). We used a prostate cell line, RWPE-1, that expresses mainly the ΔNp63 isoform (Fig. S5*A*), and a prostate carcinoma cell line (DU145), which has endogenous mutants of p53, no p63, no miR-205, and high levels of ZEB1, both at the mRNA and protein levels, compared with RWPE-1 cells (Fig. 4 *A* and *B*). In DU145 cells, ZEB1 protein levels were inhibited by 55% following transfection of precursor miR-205 (Fig. S5*B*). We next confirmed that p53 mutants inhibit p63 mRNA expression and then asked whether p53 mutants could compromise the effects of p63 on miR-205. Thus, RWPE-1 cells were transiently transfected with a p53 mutant, R175H, and transfection resulted in a significant reduction both of p63 mRNA and miR-205 expression levels (Fig. 4*C*), together with a parallel increase in ZEB1 (Fig. S5*C*) and reduced expression of p21 (Fig. S5*D*) and Bax (Fig. S5*E*) protein levels, suggesting that the mutant impaired the transcriptional activity of p63. Mutant p53 transfection also resulted in a significant reduction in miR-205 expression levels in H1299 cells transiently transfected with four different p53 mutants (Fig. S5*F*).
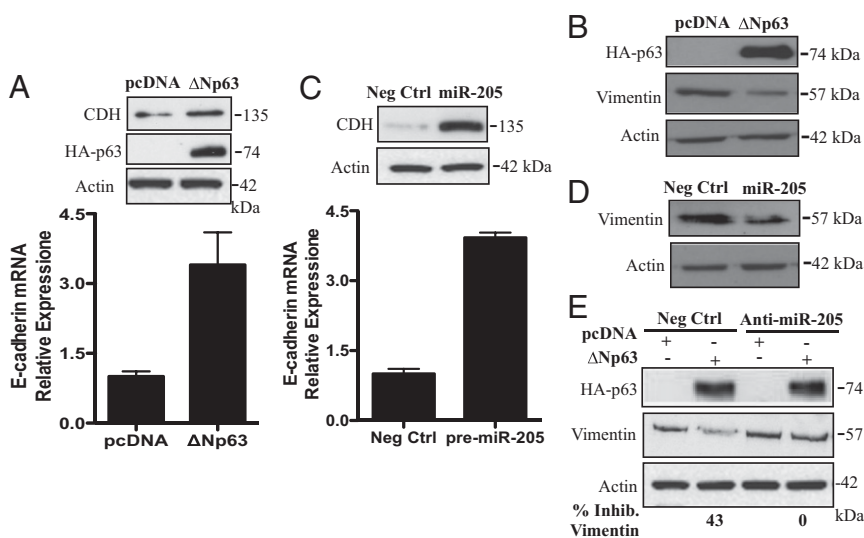

Fig. 2. ΔNp63 affects the expression of epithelial and mesenchymal markers through miR-205. PC3 cells were transfected with HA-ΔNp63 and (*A*) the expression levels of E-cadherin (CDH) were assessed by qRT-PCR and by WB, respectively, 72 and 96 h after transfection, and (*B*) levels of vimentin were assessed by WB 72 h after transfection. (*C*) PC3 cells were transfected with 50 nM pre–miR-205 or Neg Ctrl and the expression levels of CDH and (*D*) vimentin were assessed by qRT-PCR and by WB as in *A* and *B*, respectively. The qRT-PCR results were normalized to the GAPDH gene. Data represent mean ± SD of three different experiments analyzed in triplicate. (*E*) PC3 cells were treated as in Fig. 1*H* and the endogenous levels of vimentin were assessed by WB. Percentage of inhibition of vimentin protein is expressed relative to pcDNA plus Neg Ctrl and normalized to actin levels.
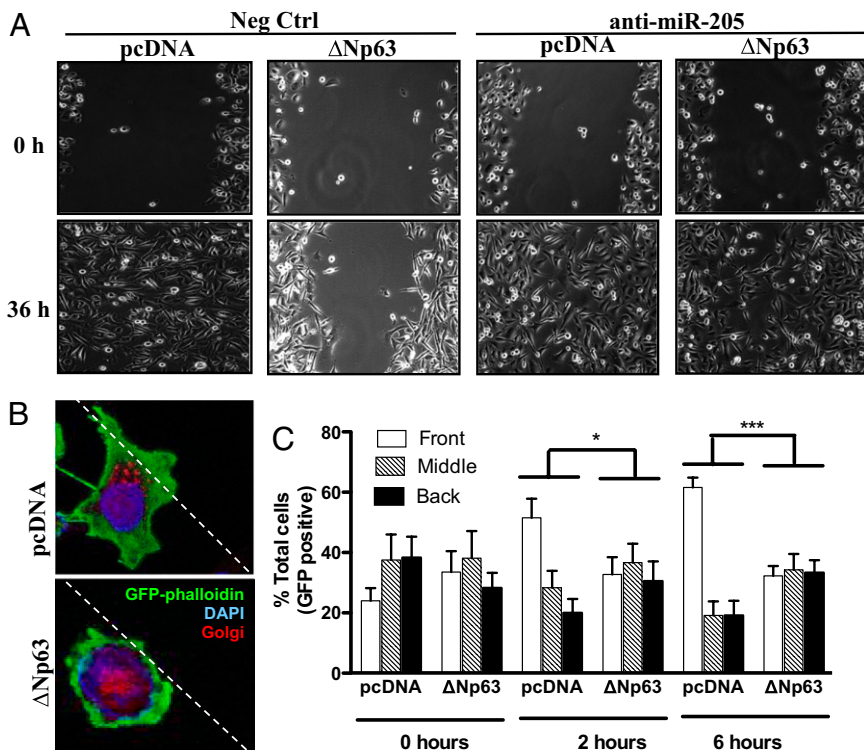
Fig. 3. ΔNp63 inhibits cell migration and polarization through miR-205. (*A*) Wound healing assays of PC3 cells transfected with HA-ΔNp63 and subsequently transfected with 100 nM anti–miR-205 or Neg Ctrl. Monolayers were scratch wounded with a p10 tip and filmed for 36 h under light time-lapse microscopy. The wound closure is illustrated by showing the wound immediately (0 h) and 36 h after the scratch. Images are representative of nine fields from three independent experiments. See also Movies S5, S6, S7, and S8. (*B*) PC3 cells, transfected with an empty vector (*Upper*) or with ΔNp63 (*Lower*) along with GFP-phalloidin (green), were grown in monolayers and wounded. Localization of the Golgi (red) was determined using immunofluorescence and cells were counterstained with DAPI (blue). Stills taken from confocal imaging and representative of three or more independent experiments are shown. (*C*) Localization of the Golgi complex in >100 GFP$^+$ cells around the edge of the wound at 0, 2, and 6 h after scratch. Data represent mean ± SEM of three different experiments analyzed in triplicate. *$P < 0.05$, ***$P < 0.001$.

To assess whether the reduction in expression of p63 targets was secondary to a reduction in the steady-state protein levels of p63 itself, we performed a cycloheximide blocking experiment measuring p63 stability. As shown in Fig. S5 *H* and *I*, p53–R175H transfection in PC3 and H1299 cells reduced p63 half-life compared with p53 WT. Conversely, knockdown of the endogenous p53 mutant in DU145 cells increased p63 stability (Fig. 4*D*, quantified in Fig. S5*G*), with an increase both of p63 protein and of its target p21 (Fig. 4*E*).

To identify a direct interaction between p53 and p63, we coimmunoprecipitated p63 and mutant p53 both in PC3 reexpressing p53-WT (Fig. 4*F* and Fig. S6 *A* and *B*) and in DU145 (Fig. S6*C*). A significant interaction was detected with all mutants, especially the DNA binding domain (DBD) unfolded R175H, a mutant known to have a destabilized DNA binding domain and being prone to aggregation (Fig. S6*D*). Coexpression in cells seems

to be necessary to establish aggregation-based interaction, whereas the more transient interaction in pull-down assays with the isolated p63 DBD is not sufficient to form stable aggregates (Fig. S6 *E* and *F*).

P53 mutant DU145 cells showed enhanced migration in the scratch assay compared with the p53 wild-type RWPE-1 cells, and this could be at least partially reversed by transfection of DU145 with pre–miR-205, and pre–miR-205 transfection in these cells had no effects on cell cycle or apoptosis (Fig. S7 *A–C* and Movies S11, S12, and S13). To further investigate the behavior of p53 mutant-expressing cells, we examined their migration in a scratch-wound assay obtained after plating DU145 cells and DU145 cells transiently transfected with a human miR-205 GFP construct (Fig. S7*D*). This confirmed that the migration of cells expressing miR-205 was inhibited. Moreover, transfected cells moved erratically into the wound (tortuosity; Fig. S7*E*),
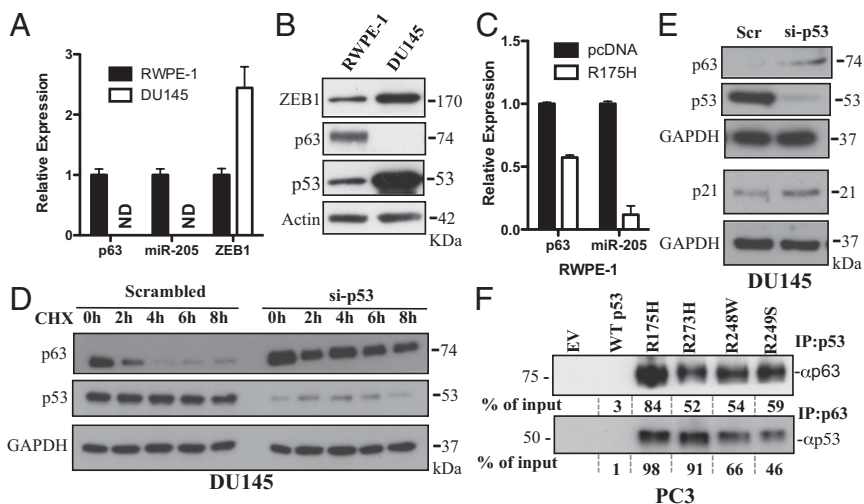

Fig. 4. Mutant p53 correlates with the loss of p63. (*A*) Expression levels of p63, miR-205, and ZEB1 in DU145 cells relative to the RWPE-1 cells. (*B*) WB of ZEB1, p63, and p53 proteins in RWPE-1 and in DU145 cell. (*C*) RWPE-1 cells were transfected with a p53 mutant, R175H, and levels of p63 and miR-205 were assessed by qRT-PCR. (*D*) Silencing of endogenous mutant p53 stabilizes p63 half-life in the presence of cycloheximide (CHX). (*E*) Reactivation of p63 protein and WB of p21 in p53-silenced DU145 cells. (*F*) p63 interacts with p53 mutants. PC3 cells were cotransfected with Myc-ΔNp63, p53 WT, or with the indicated p53 mutants and coimmunoprecipitated with the indicated antibody. Full controls are shown in Fig. S6 *A* and *B*. Percentage of pull-down over input is indicated. One of three independent experiments is shown.

Tucci et al.

displayed a marked loss of straight distance (Fig. S7F), mean velocity (Fig. S7G), and total distance migrated (Fig. S7H). Conversely, silencing of endogenous mutant p53 resulted in an inhibition of cell migration compared with the parental DU145 cells, again without affecting cell cycle profile or apoptosis (Fig. S7 I and J and Movies S14 and S15).

p63 and miR-205 Are Expressed at Lower Levels in Metastatic Prostate Cancer. To test whether the hypothesis was clinically relevant, we assessed the levels of ΔNp63 and miR-205 in biopsy samples of prostate tumors from the Taylor et al. series (20) (GSE21032) (Fig. S8G). Unsupervised clustering of samples by expression of miR-205 together with TP63 expression on all probes along its exons revealed three groups that were characterized by low expression of miR-205 and ΔNp63 (ΔNp63–miR-205 loss), high expression of miR-205, and of all probes representing ΔNp63 (ΔNp63–miR-205 function), and an intermediate group characterized by moderately low expression of ΔNp63 and mean range expression of miR-205 (ΔNp63–miR-205 intermediate). Expression of probes unique to TAp63 was insignificant in all three clusters (Fig. S8F). We found a remarkably tight correlation between the average expression of the ΔNp63 probes and miR-205 expression ($P < 1.0E-06$, Fig. 5A). Normal samples had the highest expression of both ΔNp63 and miR-205, and they all associated with the ΔNp63–miR-205 function group (Fig. 5B). Loss of both components (Fig. 5A) was significantly associated with metastatic events ($P < 1.0E-05$) and lymph node invasion ($P < 0.001$) (Fig. S8A). In addition, loss of ΔNp63 and miR-205 was associated with higher Gleason scores (Fig. S8B) and higher levels of prostate-specific antigen (PSA) (Fig. S8C). Indeed, loss of both ΔNp63 and miR-205 was found in 12 of 13 metastatic tumors and 11% of primary tumor samples. Notably, the ΔNp63–miR-205 loss group also had significantly reduced time to biochemical recurrence ($P = 1.91E-03$, Fig. 5C) and significantly

shorter overall follow-up time within the 5-y period of the study ($P = 2.97E-05$, Fig. 5D). Overall, this group clearly had the worst prognosis, whereas the ΔNp63–miR-205 function group contained all normal samples and had the best clinical prognosis.

Using EMT expression signatures (Fig. S8G), necessary because miR-205 has multiple targets, including ZEB1 (Fig. S2E) and ZEB2 (Fig. S2G) reducing statistical power, we found a clear correlation between loss of the ΔNp63–miR-205 axis and induction of EMT as indicated by these signatures (Fig. 5B), with high statistical significance (Fig. S8D).

Finally, we confirmed the impact on survival outcome in an additional dataset containing mRNA expression data from 281 prostate cancer samples from a Swedish watchful waiting cohort (21). Gene lists containing the most significantly miR-205 coexpressed genes and miR-205 antisense expressed genes were derived and gene set enrichment analysis (GSEA) was applied followed by unsupervised clustering. The resulting clusters showed that loss of ΔNp63–miR-205 function as indicated by the signatures was again predictive of poor survival ($P = 8.14E-03$, Fig. S8E). In this dataset, the EMT down-regulation signature was significantly correlated with the ΔNp63–miR-205 up-regulation signature ($P = 4.42E-03$) and inversely correlated with the ΔNp63–miR-205 down-regulation signature ($P = 9.94E-03$), suggesting suppression of EMT by an active ΔNp63–miR-205 complex.

Overall, ΔNp63–miR-205 loss was correlated with loss of epithelial markers and gain of an EMT transcriptional signature and was clearly associated with poor clinical outcome and increased metastatic potential, implying an overall functional correlation with EMT and invasive processes.

To examine whether ΔNp63 and miR-205 expression prevent tumor metastasis in vivo, we injected inducible PC3 cell lines in the tail vein of nude mice. After 3 (Fig. 5E) and 6 (Fig. S9) wk, the

Fig. 5. In human prostate cancer, loss of ΔNp63 and miR-205 associates with invasive phenotype and poor clinical outcome. Tumor and normal prostate samples clustered into three groups reflect the activity of the ΔNp63–miR-205 complex. Groups were indicative of metastatic and invasive behavior as well as clinical prognosis. (C) Time to biochemical recurrence for the three groups. (D) Clinical follow-up in the cohort was recorded over 5 y; all data are censored for survival. Kaplan–Meier analysis with suppressed censoring shows a significant trend within this follow-up time toward poor survival in the ΔNp63–miR-205 loss group. (A) miR-205/ΔNp63 relationship. Average expression of ΔNp63 was calculated from ΔNp63-specific probes and compared with miR-205 expression. Metastatic tumor samples are indicated in red diamonds, primary tumors in black squares, and normal samples in blue circles. Pearson correlation was calculated together with the significance of the correlation. Notable is the clean separation between metastatic and normal samples. (B) Heatmap illustrating miR-205 and ΔNp63 expression in prostate cancer. Data show (i) clustering of samples by their ΔNp63/miR-205 expression, Middle bars; (ii) association between normal and ΔNp63/miR-205 expression as well as metastasis and ΔNp63/miR-205 loss, Top bars; and (iii) association between the EMT signature and the expression of the ΔNp63/miR-205 axis, Bottom bars. Middle bars (clustering): Samples were clustered by their miR-205/ΔNp63 expression (red indicates significant overexpression and blue, significant underexpression of the gene/miR, true color: $P ≤ 1.0E-05$). This determined one group of samples with an active miR-205/ΔNp63 axis ("function"), one group with a clear loss of expression ("loss"), and one intermediate group ("intermediate") as indicated in the clustering bar. Top bars (primary, metastasis, normal): The group exhibiting loss of miR-205/ΔNp63 expression was enriched in metastatic samples, whereas the miR-205/ΔNp63 function group was enriched in normal tissue samples ($P < 1.0E-06$; compare also Fig. S8 A–C). Bottom bars: The miR-205/ΔNp63-loss group was also associated with an EMT transcriptional profile ($P < 0.01$, compare also Fig. S8D). Signature scores (Sarrio bars) for experimentally derived signatures according to Sarrio et al. (27) characterizing EMT are shown. Red indicates significant positive, and blue indicates significant negative association of a sample with a signature. P value for enrichment of the cluster loss with the signature EMT_up is 0.0014. Full statistics are in Fig. S8D. (E) Lung metastasis in nude mice. A total of $1.5 × 10^6$ scrambled control–PC3–Tet–On (12 mice), ΔNp63α–PC3–Tet–On (10 mice), or miR-205–PC3–Tet–On (10 mice) cells were injected through the tail vein of BALB/c nude male mice. ΔNp63α and miR-205 expression was induced with doxycycline through their drinking water. Animals were killed after 3 wk and total number of lung metastases was counted using a stereomicroscope. ***$P < 0.001$. See also Fig. S9.
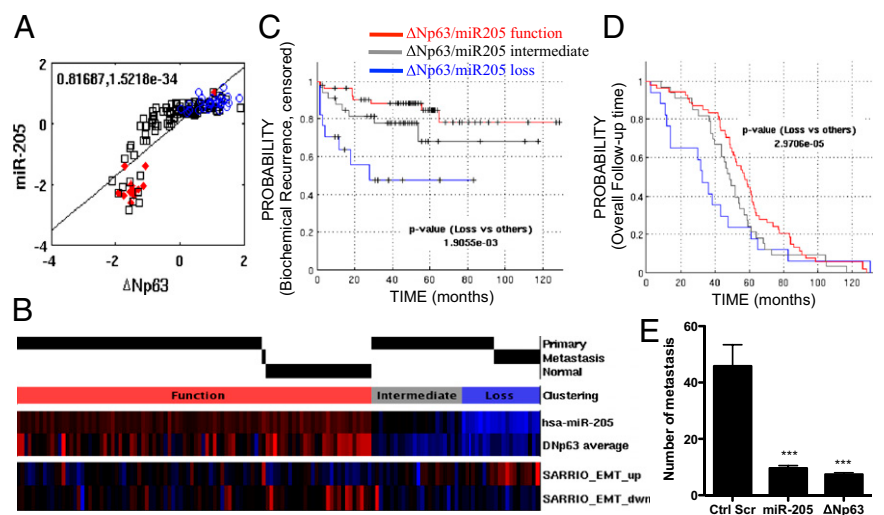
mice were killed and the lungs removed for analysis. The lungs derived from control mice injected with scrambled expressing PC3 cells had the highest number of metastases. A significant reduction in the incidence of lung metastasis was detected in mice injected with cells expressing miR-205 or ΔNp63 (Fig. 5E and Fig. S9). These results clearly show that both ΔNp63 and miR-205 expression significantly inhibit the in vivo incidence of lung metastasis.

Discussion

ΔNp63 is frequently overexpressed in epithelial cancers, being correlated with poor prognosis (22). In contrast, TAp63 has been reported to suppress metastasis through the regulation of Dicer, an enzyme important for miR maturation, and through a number of specific miRs, including miR-130b (23). In the present study, we show that miR-205 expression is regulated by both TAp63 and ΔNp63, and that both p63 and miR-205 are lost in human prostate cancer metastasis. Thus, the loss of ΔNp63 in prostate cancer is associated with metastatic spread and worse prognosis due to the indirect regulation by ΔNp63 of ZEB1, an important modulator of EMT.

Previous studies have shown that miR-205 regulates both ZEB1 and SIP1 and that inhibition of miR-205 reduces expression of E-cadherin while increasing the levels of mesenchymal markers (7). As a consequence of its involvement in the regulation of EMT, loss of miR-205 is associated with enhanced metastatic potential in both model tumor systems and in human cancers, particularly of the breast (7, 9). Several additional miR-205 targets, which may influence tumor behavior, have also been identified, including ErbB3 and VEGF-A (9), LDL receptor-related protein 1 (24), and PKCε (12). In the present study, we demonstrate that miR-205 is a direct target of ΔNp63, and the effects of ΔNp63 on EMT markers, such as ZEB1, are abrogated by anti–miR-205. Similarly, the inhibition of cell migration resulting from ΔNp63 expression is reversed by anti–miR-205. In human prostate cancer samples, partial, and more strikingly, complete loss of the ΔNp63/miR-205 axis is correlated with EMT expression patterns and is a predictor of metastatic spread, lymph node involvement, and overall poor prognosis.

p53 mutants have been shown to physically interact with p63 isoforms (25, 26). TAp63 and ΔNp63 activity can also be inhibited when they are incorporated into a complex with mutant p53 and TGFβ activated Smads, with dysregulation of two metastasis-related genes, Sharp-1 and cyclin G2 (15). In the present study, we show that p53 mutants reduce ΔNp63 and miR-205 expression in cells, with a corresponding increase in cell migration. This is at least partially rescued by transfection with pre–miR-205. We further demonstrate that several p53 mutants, reduce p63 stability, and the reduction in p63 levels may contribute to the reduced expression of its transcriptional targets such as miR-205. However, we cannot exclude the possibility that mutant p53 also inhibits p63 activity by competition for consensus binding sites in the promoters of target genes or by sequestration into aggregates. Thus, in cancers in which p53 mutations tend to occur in late stages, cell migration, EMT, and metastasis could all be potentially enhanced, even when p63 remains expressed, due to its functional inhibition by mutant p53.

These data show that the p63/miR-205 axis provides a linked molecular footprint, which is predictive of the metastatic potential of prostate cancer, and which may be a useful clinical biomarker. In addition, studies aimed at identifying the mechanisms that lead to ΔNp63 down-regulation in the prostate, such as miR-203, may reveal new therapeutic targets to contain the spread of this common cancer.

Materials and Methods

Details are provided in SI Materials and Methods for cell culture and transfection, generation of stable cell lines, Western blotting, coimmunoprecipitation, RNA extraction, qRT-PCR, Luc assay, chromatin immunoprecipitation, wound healing assay, immunofluorescence microscopy, flow cytometry analysis, gene expression and clustering analysis, and tumor metastasis in vivo.

Data are reported as mean values ± SD or ± SEM of at least three independent experiments. Unpaired Student t test was used to generate statistical analysis. P values <0.05 were considered statistically significant.

1. Yang A, et al. (1998) p63, a p53 homolog at 3q27-29, encodes multiple products with transactivating, death-inducing, and dominant-negative activities. Mol Cell 2: 305–316.
2. Levine AJ, Tomasini R, McKeon FD, Mak TW, Melino G (2011) The p53 family: Guardians of maternal reproduction. Nat Rev Mol Cell Biol 12:259–265.
3. Melino G (2011) p63 is a suppressor of tumorigenesis and metastasis interacting with mutant p53. Cell Death Differ 18:1487–1499.
4. Antonini D, et al. (2010) Transcriptional repression of miR-34 family contributes to p63-mediated cell cycle progression in epidermal cells. J Invest Dermatol 130: 1249–1257.
5. Rivetti di Val Cervo P, et al. (2012) p63-microRNA feedback in keratinocyte senescence. Proc Natl Acad Sci USA 109:1133–1138.
6. Gregory PA, Bracken CP, Bert AG, Goodall GJ (2008) MicroRNAs as regulators of epithelial-mesenchymal transition. Cell Cycle 7:3112–3118.
7. Gregory PA, et al. (2008) The miR-200 family and miR-205 regulate epithelial to mesenchymal transition by targeting ZEB1 and SIP1. Nat Cell Biol 10:593–601.
8. Baffa R, et al. (2009) MicroRNA expression profiling of human metastatic cancers identifies cancer gene targets. J Pathol 219:214–221.
9. Wu H, Zhu S, Mo YY (2009) Suppression of cell growth and invasion by miR-205 in breast cancer. Cell Res 19:439–448.
10. Coppola V, De Maria R, Bonci D (2010) MicroRNAs and prostate cancer. Endocr Relat Cancer 17:F1–F17.
11. Majid S, et al. (2010) MicroRNA-205-directed transcriptional activation of tumor suppressor genes in prostate cancer. Cancer 116:5637–5649.
12. Gandellini P, et al. (2009) miR-205 Exerts tumor-suppressive functions in human prostate through down-regulation of protein kinase Cepsilon. Cancer Res 69: 2287–2295.
13. Graham TR, et al. (2008) Insulin-like growth factor-I-dependent up-regulation of ZEB1 drives epithelial-to-mesenchymal transition in human prostate cancer cells. Cancer Res 68:2479–2488.
14. Kupfer A, Louvard D, Singer SJ (1982) Polarization of the Golgi apparatus and the microtubule-organizing center in cultured fibroblasts at the edge of an experimental wound. Proc Natl Acad Sci USA 79:2603–2607.
15. Adorno M, et al. (2009) A Mutant-p53/Smad complex opposes p63 to empower TGFbeta-induced metastasis. Cell 137:87–98.
16. Muller PAJ, et al. (2009) Mutant p53 drives invasion by promoting integrin recycling. Cell 139:1327–1341.
17. Lang GA, et al. (2004) Gain of function of a p53 hot spot mutation in a mouse model of Li-Fraumeni syndrome. Cell 119:861–872.
18. Flores ER, et al. (2005) Tumor predisposition in mice mutant for p63 and p73: Evidence for broader tumor suppressor functions for the p53 family. Cancer Cell 7:363–373.
19. Muller PA, et al. (2012) Mutant p53 enhances MET trafficking and signalling to drive cell scattering and invasion. Oncogene, 10.1038/onc.2012.148.
20. Taylor BS, et al. (2010) Integrative genomic profiling of human prostate cancer. Cancer Cell 18:11–22.
21. Sboner A, et al. (2010) Molecular sampling of prostate cancer: A dilemma for predicting disease progression. BMC Med Genomics 16:3–8.
22. Chiang CT, Chu WK, Chow SE, Chen JK (2009) Overexpression of delta Np63 in a human nasopharyngeal carcinoma cell line downregulates CKIs and enhances cell proliferation. J Cell Physiol 219:117–122.
23. Su X, et al. (2010) TAp63 suppresses metastasis through coordinate regulation of Dicer and miRNAs. Nature 467:986–990.
24. Song H, Bu G (2009) MicroRNA-205 inhibits tumor cell migration through downregulating the expression of the LDL receptor-related protein 1. Biochem Biophys Res Commun 388:400–405.
25. Strano S, et al. (2002) Physical interaction with human tumor-derived p53 mutants inhibits p63 activities. J Biol Chem 277:18817–18826.
26. Gaiddon C, Lokshin M, Ahn J, Zhang T, Prives C (2001) A subset of tumor-derived mutant forms of p53 down-regulate p63 and p73 through a direct interaction with the p53 core domain. Mol Cell Biol 21:1874–1887.
27. Sarrió D, et al. (2008) Epithelial-mesenchymal transition in breast cancer relates to the basal-like phenotype. Cancer Res 68:989–997.

CELL BIOLOGY